ACCSCIENCE PUBLISHING

Materials Science in Additive Manufacturing

ORIGINAL RESEARCH ARTICLE

Hybrid resorbable anchors/biomolecule-eluting nanofibers for enhanced pedicle screw fixation

Po-Ju Lai[1,2], Chih-Yang Lai[1,2], Chien-Yun Yang[1], I-Lan Fan[1], Ching-Lung Tai[1], and Shih-Jung Liu[1,2]*

[1]Department of Mechanical Engineering, Chang Gung University, Taoyuan, Taiwan

[2]Bone and Joint Research Center, Department of Orthopedics, Chang Gung Memorial Hospital at Linkou, Taoyuan, Taiwan

Abstract

Pedicle screw loosening remains a challenge for surgeons and patients. We propose using hybrid resorbable anchors and drug/biomolecule-eluting nanofibers to enhance the bone fixation of pedicle screws. Polylactide (PLA) anchors with various designs were fabricated using additive manufacturing, while simvastatin- and bone morphogenetic protein-2 (BMP-2)-loaded poly(lactic-co-glycolic acid) (PLGA) nanofibers were prepared through coaxial electrospinning. The effects of PLA anchors and drug/biomolecule-loaded PLGA nanofibrous membranes on improving the pullout strength of pedicle screws from artificial bones were investigated. The *in vitro* release characteristics of simvastatin and BMP-2 from the nanofibers were evaluated using high-performance liquid chromatography and enzyme-linked immunosorbent assay, while the *in vivo* elution of simvastatin was assessed in a rabbit model with histological examinations. The results demonstrate that electrospun drug/biomolecule-eluting nanofibers, when wrapped around pedicle screws, enhance the screws' pullout strength. Additionally, the nanofiber/screw system provides a sustained release of simvastatin and BMP-2 for over 30 days *in vitro* and 4 weeks *in vivo*. Histological analysis also confirmed the biocompatibility of nanofibrous anchors. Hybrid resorbable anchors and drug/biomolecule-eluting nanofibers show potential for improving screw fixation and serving as a platform for extended drug delivery.

Keywords: Additive manufacturing; Resorbable anchor; Electrospinning; Drug-eluting nanofibers; Screw fixation

***Corresponding author:**
Shih-Jung Liu
(shihjung@mail.cgu.edu.tw)

Citation: Lai P-J, Lai C-Y, Yang C-Y, Fan I-L, Tai C-L, Liu S-J. Hybrid resorbable anchors/biomolecule-eluting nanofibers for enhanced pedicle screw fixation. *Mater Sci Add Manuf.* doi: 10.36922/MSAM026340083

Received: August 18, 2026

Revised: September 22, 2026

Accepted: September 29, 2026

Published online: November 2, 2026

Copyright: © 2026 Author(s). This is an Open-Access article distributed under the terms of the Creative Commons Attribution License, permitting distribution, and reproduction in any medium, provided the original work is properly cited.

Publisher's Note: AccScience Publishing remains neutral with regard to jurisdictional claims in published maps and institutional affiliations.

1. Introduction

Instability and loosening of pedicle screws pose a major clinical hurdle, particularly during long-segment spinal reconstructions or in patients with compromised bone quality. Unstable instrumentation often triggers severe persistent pain, functional disability, hardware breakdown, and secondary surgical interventions.[1] Despite technological advancements, screw-loosening rates vary from under 15% in healthy bone to as high as 60% in osteoporotic vertebrae. Key risk factors include advanced patient age, systemic osteoporosis, multi-level fusion constructs, elevated pelvic incidence, and under-corrected sagittal balance (pelvic incidence–lumbar lordosis mismatch > 10°).[2,3]

Decreased bone mineral density reduces pullout forces and insertion torque, whereas long-segment fixations impose substantial mechanical loads on the screw–bone junction. Notably, degenerative lumbar scoliosis carries a higher prevalence of low bone mass, predisposing these individuals to elevated loosening rates following fusion.[1,4-5]

Management of mild screw loosening often relies on conservative brace immobilization to minimize micro-motion at the implant interface. For moderate-to-severe instability, mechanical augmentation techniques are routinely employed. Polymethylmethacrylate (PMMA) bone cement injection represents the predominant surgical strategy to fortify screw anchorage.[6,7] In refractory cases, revision procedures using larger-diameter or longer hardware are necessary to regain mechanical purchase.[8] Resolving these issues necessitates innovative approaches, including geometry optimization, interface functionalization, and localized therapeutic agent delivery to stimulate bone formation and reduce local inflammation.

Alternative mechanical solutions have been explored. McKoy and An[9] introduced an expanding anchoring device designed to increase pullout resistance in weak trabecular bone without bone cement. However, forced radial expansion can cause severe local structural damage to fragile osteoporotic bone. Fenestrated screws designed for PMMA delivery offer another alternative,[10] yet PMMA remains prone to monomer cytotoxicity, exothermic thermal injury, cement extravasation, and indefinite permanence *in vivo*.[6,10] Consequently, resorbable polymeric augments have gained increasing attention to improve initial screw stability while enabling subsequent physiological bone ingrowth.[11,12]

A screw anchor is a fastener used to attach objects to walls or other materials that are not strong enough to hold the object securely.[13] Screw anchors are inserted into a pre-drilled hole and expand when the screw is driven in, creating a secure hold in drywall, plaster, or masonry. They distribute the weight and force over a larger area, preventing the screw from pulling out or damaging the wall material. Polymeric screw anchors are the most common type, used for lightweight applications.

This study proposes the use of hybrid resorbable anchors and drug-eluting nanofibers to enhance the bone fixation of pedicle screws and evaluates their effectiveness. Polylactide (PLA) anchors of various designs were fabricated using additive manufacturing, while simvastatin-loaded and bone morphogenetic protein-2 (BMP-2)-loaded poly(lactic-co-glycolic acid) (PLGA) nanofibers were produced using coaxial electrospinning.

The effects of PLA anchors and drug/biomolecule-loaded PLGA nanofibrous membranes on improving the pullout strength of pedicle screws from artificial bones were investigated using a tensile tester. The *in vitro* release characteristics of simvastatin and BMP-2 from the nanofibers were evaluated using high-performance liquid chromatography (HPLC) and enzyme-linked immunosorbent assay (ELISA). Additionally, the *in vivo* elution of simvastatin was assessed in a rabbit model through histological examinations.

2. Materials and methods

2.1. Materials

The polymeric materials used were PLA filament and 50:50 PLGA (RG503, Mw 24,000–38,000). The biomolecules included simvastatin and BMP-2. The solvent used was 1,1,1,3,3,3-hexafluoro-2-propanol (HFIP). The PLA filament was purchased from Prolink Microsystems Corp. (Taiwan), while the other materials were obtained from Sigma-Aldrich (United States of America [USA]).

2.2. Additive manufacturing of polylactide anchors

Two anchor designs were proposed, with the dimensions and layout of the anchors shown in Figure 1A. To manufacture the anchors, PLA filaments and a fused deposition modeling printer (V2-B Dual Extruder Printer, Kraftmaker, Taiwan) were employed. The entire fabrication process was controlled using the Ultimaker Cura software (Version 4.8, Ultimaker B.V., The Netherlands). Figure 1B displays the fabricated PLA anchors.

2.3. Coaxial electrospinning of nanofibrous membranes

Core–shell nanofibrous membranes were produced using a custom coaxial electrospinning setup equipped with dual concentric feeding channels.[14] The sheath formulation was prepared by dissolving PLGA (630 mg) and simvastatin (210 mg) in 3 mL of HFIP, whereas the core phase contained BMP-2 (20 μg), bovine serum albumin (1 mL), and phosphate-buffered saline (PBS; 1 mL). Both solutions were loaded into separate syringe pumps, with volumetric flow rates set at 0.3 mL/h for the PLGA/simvastatin shell and 0.1 mL/h for the BMP-2 core. Electrospinning was conducted at an applied voltage of 18 kV across a 15 cm working distance onto a grounded collector. Single-fluid electrospun PLGA fibers were fabricated under identical conditions for comparison. All processes were performed at ambient temperature, producing meshes with an average thickness of ~110 μm, which were subsequently vacuum-dried at 40 °C for 72 h to eliminate residual HFIP.

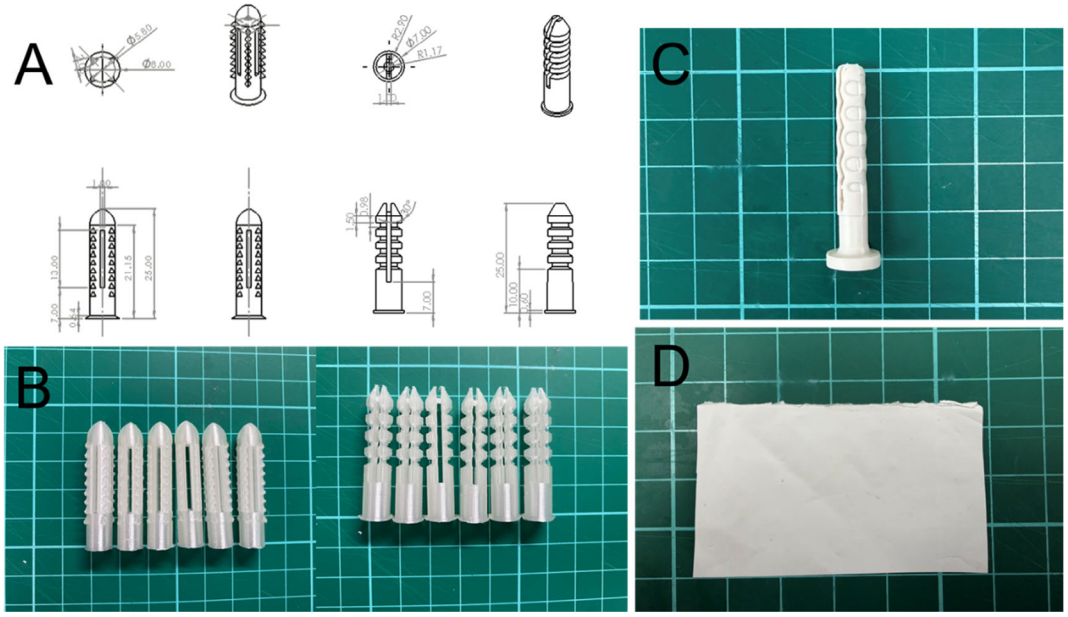


Figure 1. Fabrication and design of hybrid resorbable anchors and drug-loaded nanofibers. (A) Dimensions and layout of the anchors, (B) 3D-printed anchors, (C) a commercial nylon anchor, and (D) electrospun drug-loaded nanofibers.

2.4. Characterization of spun membranes

The morphology of virgin nanofibers and the PLGA/simvastatin/BMP-2 nanofibers were characterized after gold coating under a scanning electron microscope (SEM; JSM-7500F, Jeol, Japan).

To provide direct evidence of macromolecular protein (BMP-2) incorporation and to visualize its spatial distribution within the core–shell structure, recombinant enhanced green fluorescent protein (reGFP; molecular weight ~27 kDa; Sigma-Aldrich, Germany), used as a fluorescent surrogate for BMP-2, was encapsulated in the core mixture during coaxial electrospinning. The resulting fibers were observed using a laser scanning confocal microscope (TS SP8X, Leica, Japan) at an excitation wavelength of 487 nm.

The water contact angles of manufactured nanofibers were determined through a water contact angle analyzer (FTA1000, First Ten Angstroms, USA). Samples measuring 1 cm × 1 cm were obtained from the membranes and positioned on the testing plate. Distilled water was then dropped carefully on their surfaces. The contact angles were assessed using a video monitor.

A Nicolet iS5 Fourier transform infrared (FTIR) spectrometer (Thermo Fisher, USA) was used to characterize the spectra of both pristine and drug/molecule-embedded nanofibers at a resolution of 4 cm^{-1} and 32 scans. PLGA were compressed into potassium bromide discs, and spectra were monitored over the 400–4,000 cm^{-1} range.

Differential scanning calorimetry was used to analyze the thermal profiles of pristine PLGA and drug/molecule-incorporated PLGA nanofibers. The analysis was carried out using a model DSC25 instrument (TA Instruments, USA), with a scanning temperature range of 30 °C–250 °C and a heating rate of 10 °C/min.

2.5. Pullout strengths

The pedicle screw had a thread depth of 1.0 mm, a thread pitch of 1.5 mm, and a standard thread coverage length of 40 mm. To mimic the cortical and cancellous components of osteoporotic bone, two synthetic test blocks (Pacific Research Laboratory Inc., USA) with different structures and mechanical properties were used: solid rigid foam (Model 1522-02) to represent the dense cortical bone component and open-cell rigid foam (Model 1522-524) to represent the more porous cancellous bone component.

The specimens were categorized into five groups. Group 1 included bare pedicle screws. Group 2 involved the insertion of the PLA-1 anchor, followed by the pedicle screw (Figure 2B). In Group 3, screws were fixed along with the PLA-2 anchor (Figure 2B). Group 4 utilized a

commercially available nylon anchor (Figure 1C) inserted into the test block, followed by pedicle screw fixation. In Group 5, pedicle screws were wrapped with drug-eluting nanofibers (Figure 1D).

The test blocks were prepared with dimensions of 50 mm × 50 mm × 80 mm. For bare screws, a 4.0 mm cylindrical hole was drilled into the test block, and the screw (with or without mesh or nanofibers) was inserted until all threads were fully embedded (Figure 2A). For the nylon anchor and PLA anchors, 5.0 mm and 6.0 mm holes were drilled before inserting the screws.

The pullout strengths of pedicle screws, both alone and with different resorbable anchors, were measured using a laboratory-made fixture (Figure 2B) mounted on a tensile test machine (Model E10000/E10BMTB19359, Instron, USA). The fixture could automatically align itself to ensure the screw's long axis was coaxial with the test machine. During the test, the specimen was subjected to a rate of 5 mm/min while being pulled by the top clamp. The maximum load and elongation were recorded. Measurements were performed in triplicate (n = 3) for each screw.

2.6. *In vitro* release patterns of biomolecules

The release kinetics of simvastatin and BMP-2 from the electrospun matrices were quantified using an *in vitro* dissolution protocol. Membrane specimens (10 mm × 10 mm; n = 3) were immersed in test tubes containing 1 mL of PBS (pH 7.4, 0.15 M) and maintained at 37 °C. At 24-h intervals over 30 consecutive days, the complete supernatant was collected for analysis and replenished with an equal volume of fresh PBS. Simvastatin concentrations were quantified using HPLC (L-2200R multisolvent system, Hitachi, Japan) equipped with a C18 column (250 × 4.6 mm, 5 μm) and a UV detector set at 238 nm, utilizing an acetonitrile/sodium dihydrogen phosphate mobile phase (65:35 v/v) at a flow rate of 1.0 mL/min.[15] Released BMP-2 levels were determined via a commercial ELISA kit (RAB0028, Sigma-Aldrich, USA).

2.7. Cytotoxicity of electrospun nanofibers

Evaluation of basic cellular compatibility was performed via the 3-(4,5-dimethylthiazol-2-yl)-2,5-diphenyltetrazolium bromide (MTT) colorimetric assay (XXX, YYY, ZZZ) in compliance with ISO 10993-5 standards. Eluates collected from nanofiber samples were added to cultures of L929 fibroblasts (Bioresource Collection and Research Center, Food Industry Research and Development Institute, Taiwan) seeded in 24-well plates at an initial density of 5 × 10^3 cells/well. Cells were cultured in Dulbecco's modified Eagle medium (Gibco, USA), supplemented with 10% (v/v) fetal bovine serum (Gibco, USA) and 1% (v/v) penicillin–streptomycin solution (100 U/mL penicillin and 100 μg/mL streptomycin; Gibco, USA). Cells were incubated under humidified 5% CO_2 conditions at 37 °C. At post-exposure days 1, 3, 7, and 14, metabolic activity was assessed by measuring optical density at 570 nm using a microplate spectrophotometer.

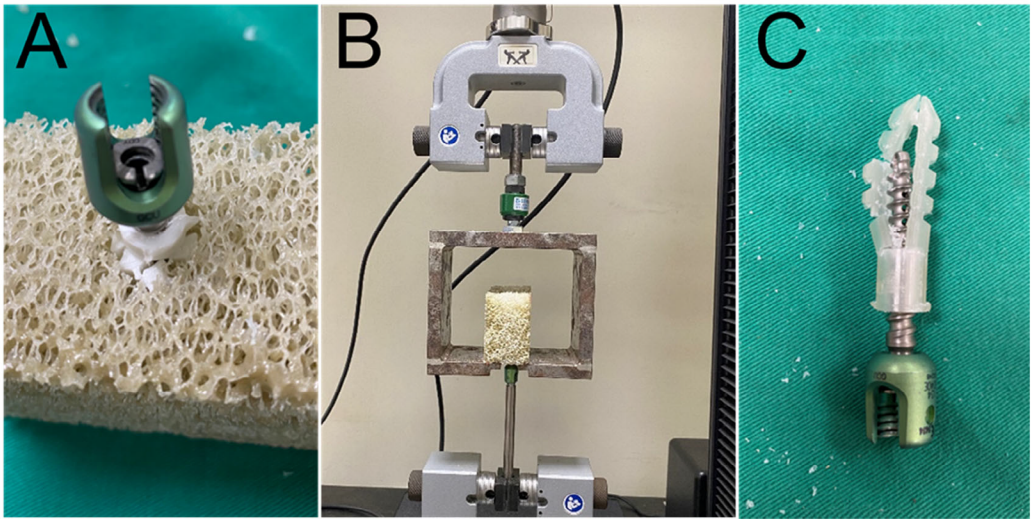


Figure 2. Biomechanical pullout test setup and insertion failure mode of 3D-printed polylactide (PLA) anchors. (A) Fixation of the anchored screw in the artificial bone, (B) fixture used for pullout tests, and (C) representative longitudinal fracture mode of 3D-printed PLA anchors during testing.

2.8. *In vivo* release

New Zealand rabbits (2,500–3,000 g, male, approximately 1.2 years old; n = 5; obtained from the Taiwan Livestock Research Institute, Ministry of Agriculture, Taiwan) were used in this study. All animal procedures and protocols were performed in strict accordance with the guidelines and were approved by the Institutional Animal Care and Use Committee (IACUC) of Chang Gung University, Taoyuan, Taiwan (Approval No.: CGU113-030).

A screw with a thread depth of 1.0 mm, a thread pitch of 1.5 mm, and a standard thread coverage length of 40 mm was used. Prior to implantation, simvastatin/BMP-2-incorporated nanofibers were wrapped around the surface of the screws. The animals were anesthetized with isoflurane inhalation and maintained with a mask throughout the surgical procedure. After induction of anesthesia, a skin incision over the lateral thigh was made, and an approach through intermuscular planes to the right femur was made (Figure 3A). The drug/biomolecule-loaded screw was then inserted into the right femur (Figure 3B), and the surgical wound was closed in layers (Figure 3C).

In vivo drug concentrations were evaluated by collecting tissue and blood samples from the surgical site at 1, 3, 7, 14, 21, and 28 days post-implantation. The samples were analyzed using HPLC (n = 3). Additionally, tissue samples surrounding the implants were harvested for qualitative histological analysis to assess local biocompatibility and tissue response.

2.9. Statistics and data analysis

Three independent specimens were analyzed per group using one-way analysis of variance. A p-value of less than 0.05 was considered statistically significant.

3. Results

3.1. Pullout strengths of screws and anchors

The pullout strengths of the pedicle screws and anchors were measured. Figure 4A and 4B presents the results obtained from tests conducted on simulated cortical and cancellous bone, respectively. In cortical bone, the bare screws exhibited the highest initial fixation strength, with peak forces of approximately 1,100 N, followed closely by screws coated with nanofibers (~1,000 N). Although the screw/nylon anchor system showed a lower peak load (~700–800 N), it maintained noticeably higher forces with increasing displacement, indicating improved post-yield stability and resistance to progressive loosening. In contrast, both PLA anchors (PLA-1 and PLA-2) exhibited substantially lower peak forces (~300–400 N) and more rapid force decay as displacement increased. This may be attributed to fracture of the PLA anchors after insertion of the pedicle screws (Figure 2C). As a result, the pullout strengths were reduced accordingly.

In cancellous bone, the screw/nanofiber group showed the highest pullout strength, demonstrating the capability of the nanofibers to enhance the pullout strength of pedicle screws. Once again, screws combined with PLA anchors exhibited the lowest pullout strengths.

3.2. Characterization of drug/biomolecule loaded nanofibers

Both pristine PLGA and drug/biomolecule-loaded core–shell-structured PLGA nanofibers were successfully fabricated using electrospinning and co-electrospinning techniques. Figure 5A and 5B displays their SEM micrographs. The measured average diameters were 556 ± 202 nm for pristine PLGA nanofibers and 1,682 ± 852 nm for core–shell-structured PLGA nanofibers, with all fibrous membranes exhibiting high porosity.

To directly confirm the successful loading and core–shell spatial distribution of the protein biomolecules (BMP-2), laser scanning confocal microscopy was performed using reGFP as a macromolecular tracer. As shown in the confocal fluorescent micrograph (Figure 5B), distinct, continuous, string-like green fluorescence

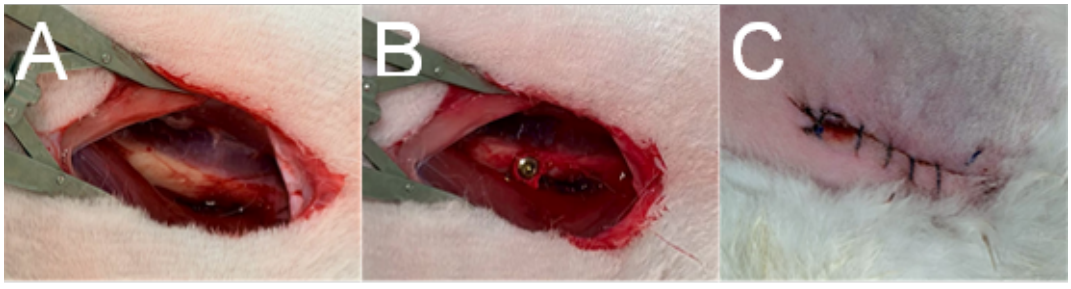


Figure 3. Implantation procedure of the screws wrapped with drug-loaded nanofibers. (A) Incision over the lateral thigh and dissection through intermuscular planes to the femur, (B) the drug/biomolecule-loaded screw was then inserted into the right femur, and (C) skin closure.

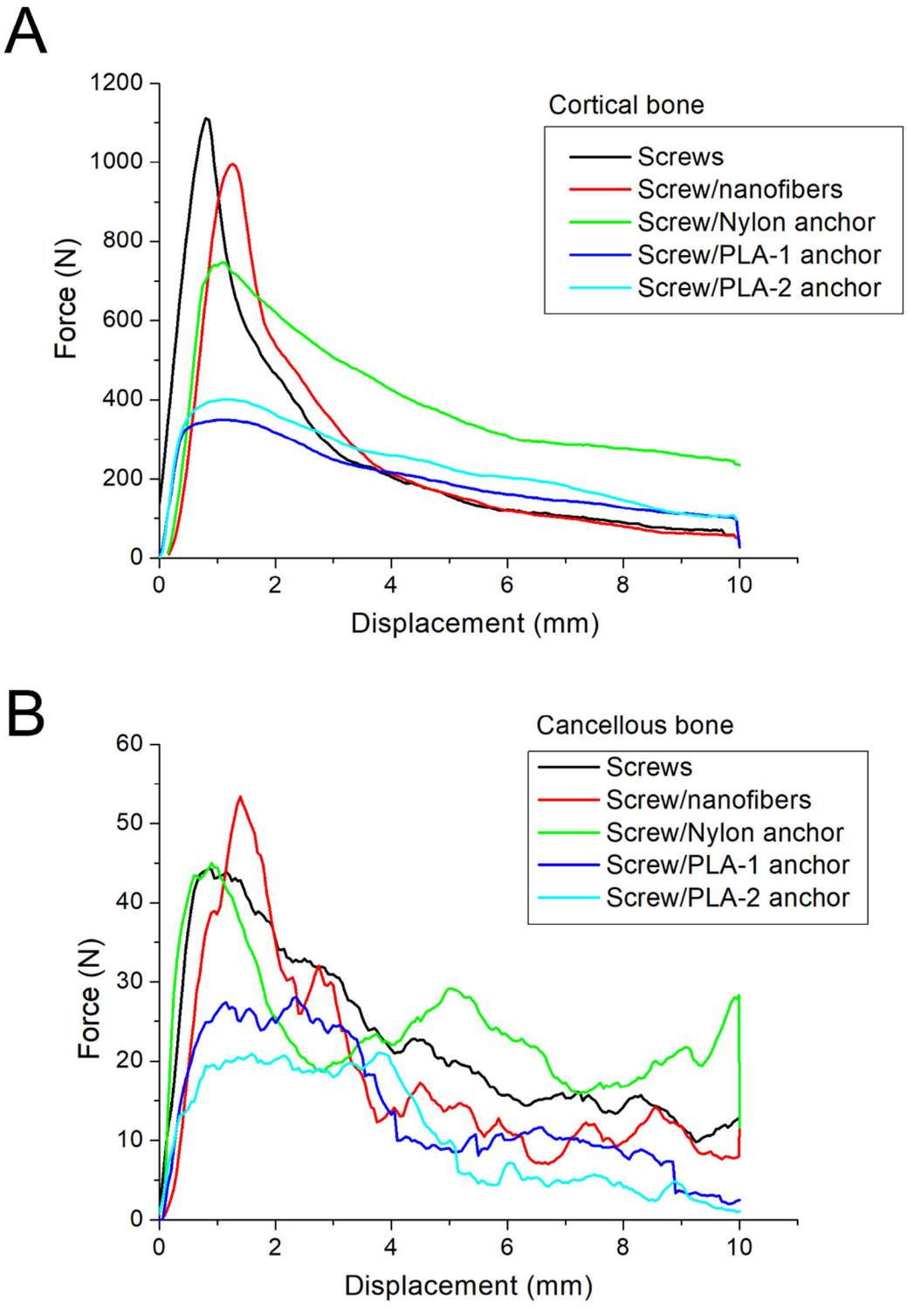


Figure 4. Pullout strengths of pedicle screws in artificial (A) cortical bone and (B) cancellous bone

signals were clearly localized along the inner core of the PLGA nanofibers. This visual evidence directly verifies that biomacromolecules were successfully encapsulated into the core structure via coaxial electrospinning while maintaining their structural integrity.

The wetting angles of pristine PLGA and core–shell simvastatin/BMP-2-loaded PLGA nanofibers are shown in **Figure 6**, measuring 136.4° and 100.6°, respectively. The incorporation of the semi-water-soluble simvastatin in the sheath layer enhanced the hydrophilic characteristics of the fabricated nanofibers.

The mechanical strengths of the manufactured nanofibers were investigated. The tensile strength results shown in Figure 7 indicate that the ultimate strength and extensibility of the drug-loaded nanofibers decreased with the addition of drugs/biomolecules. In a polymer/drug composite, the polymer primarily resists external forces. As the drug content increased, the polymer content in the electrospun composite mesh decreased, leading to a reduction in mechanical strength.

Figure 8A presents the FTIR spectra of pristine PLGA and pharmaceutical-incorporated PLGA nanofibers. The new vibration peak at 1,650 cm^{-1} is attributed to the C=C bonds of the aromatic rings in simvastatin.[16] Figure 8B compares the thermal behaviors of pristine PLGA and biomolecule-loaded PLGA nanofibers. After simvastatin was incorporated into the PLGA matrix, the endothermic peak at 138 °C significantly diminished.[17] These results confirm the successful incorporation of simvastatin into the PLGA nanofibrous scaffolds.

3.3. *In vitro* release of simvastatin and bone morphogenetic protein 2 from biodegradable nanofibers

The release of simvastatin from the electrospun core–shell structured nanofibers was characterized. Figure 9A and 9B shows the release profiles of simvastatin and BMP-2, respectively, over a 30-day period. The simvastatin profile begins with a pronounced burst release, reaching concentrations near 200 µg/mL on day 1. After this peak,

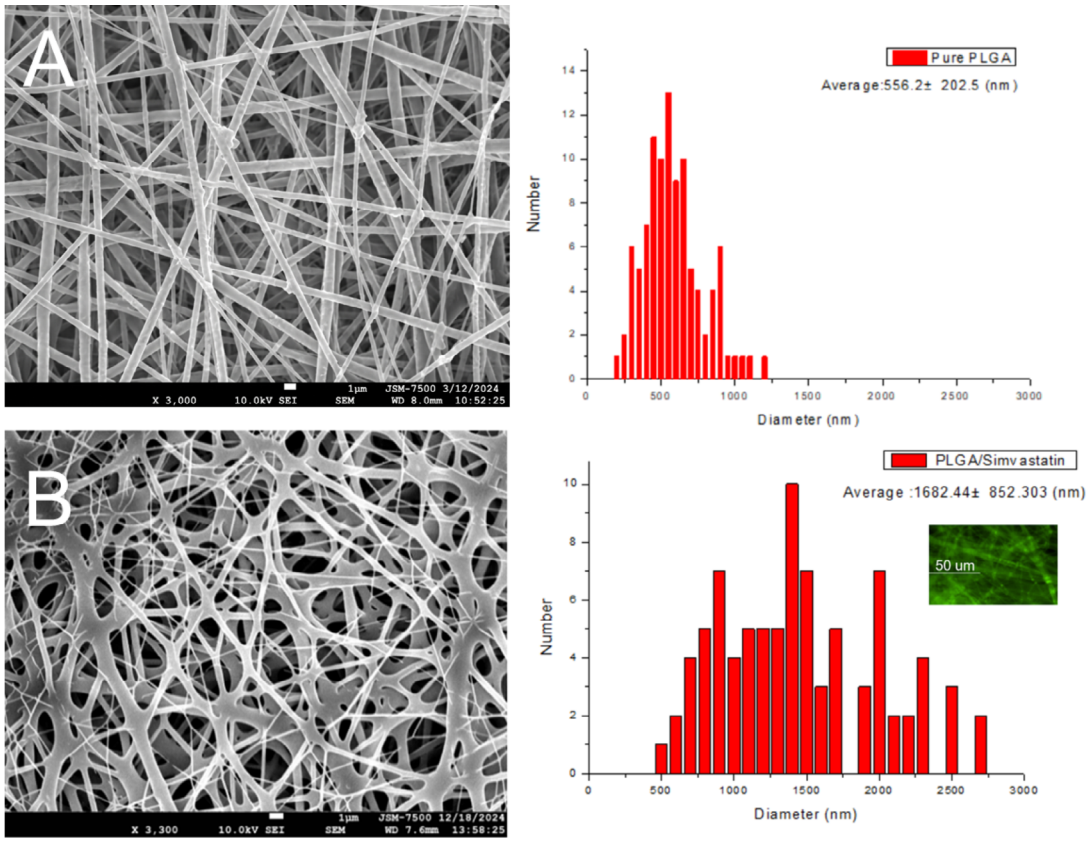


Figure 5. Scanning electron microscopy image and fiber size distribution of (A) pure poly(lactic-co-glycolic acid) (PLGA) nanofibers (scale bar: 1 µm; magnification: 3,000×) and (B) simvastatin and bone morphogenetic protein 2 (BMP-2)-loaded nanofibers (scale bar: 1 µm; magnification: 3,300×). The inset in (B) shows a fluorescence microscopy image (scale bar: 50 µm; magnification: 400×).

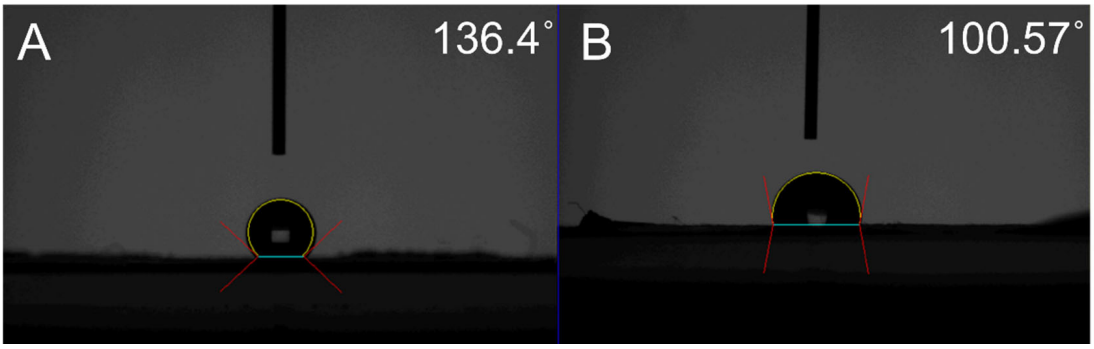


Figure 6. Water contact angles of (A) pure poly(lactic-co-glycolic acid) nanofibers and (B) simvastatin and bone morphogenetic protein 2-loaded nanofibers

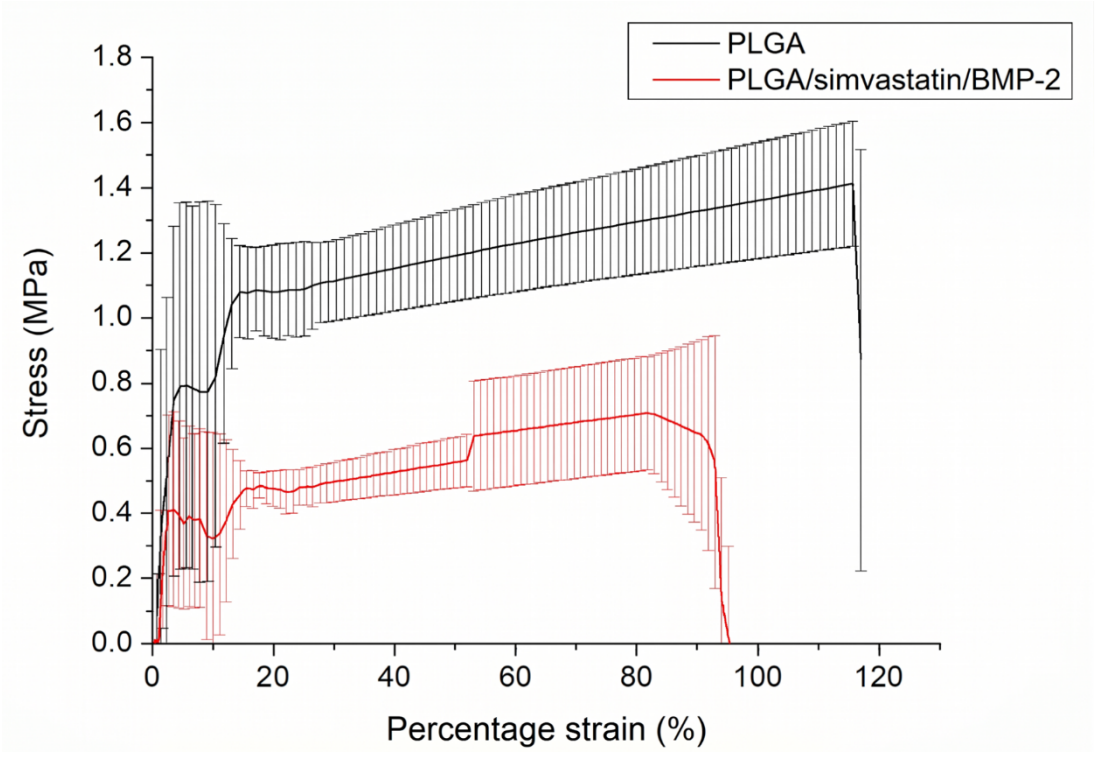


Figure 7. Stress–strain curves of pure poly(lactic-co-glycolic acid) (PLGA) and simvastatin/bone morphogenetic protein 2 (BMP-2)-loaded PLGA nanofibers

the concentration drops sharply over the next several days, falling below 10 μg/mL by approximately day 6. For the remainder of the study, the release follows a low-level sustained pattern, fluctuating roughly between 1 and 10 μg/mL with small variations and occasional brief peaks. Overall, the drug-loaded nanofibers were able to elute simvastatin for over 30 days. Meanwhile, the measured profile in Figure 9B shows that the core–shell structured nanofibers could provide sustained and stable release of BMP-2, at around 50–80 pg/mL, for over 30 days. There is no dramatic drop-off, demonstrating stable long-term delivery of the molecule. Additionally, the cytotoxicity analysis results shown in Figure 10 demonstrate that the drug-eluting nanofibers exhibit no detectable cytotoxicity.

3.4. *In vivo* elution

The *in vivo* release profile shown in Figure 11 indicates that the drug-eluting nanofibers can sustain high levels of local simvastatin release for 28 days in the tissues surrounding the implanted membranes, despite low systemic drug levels

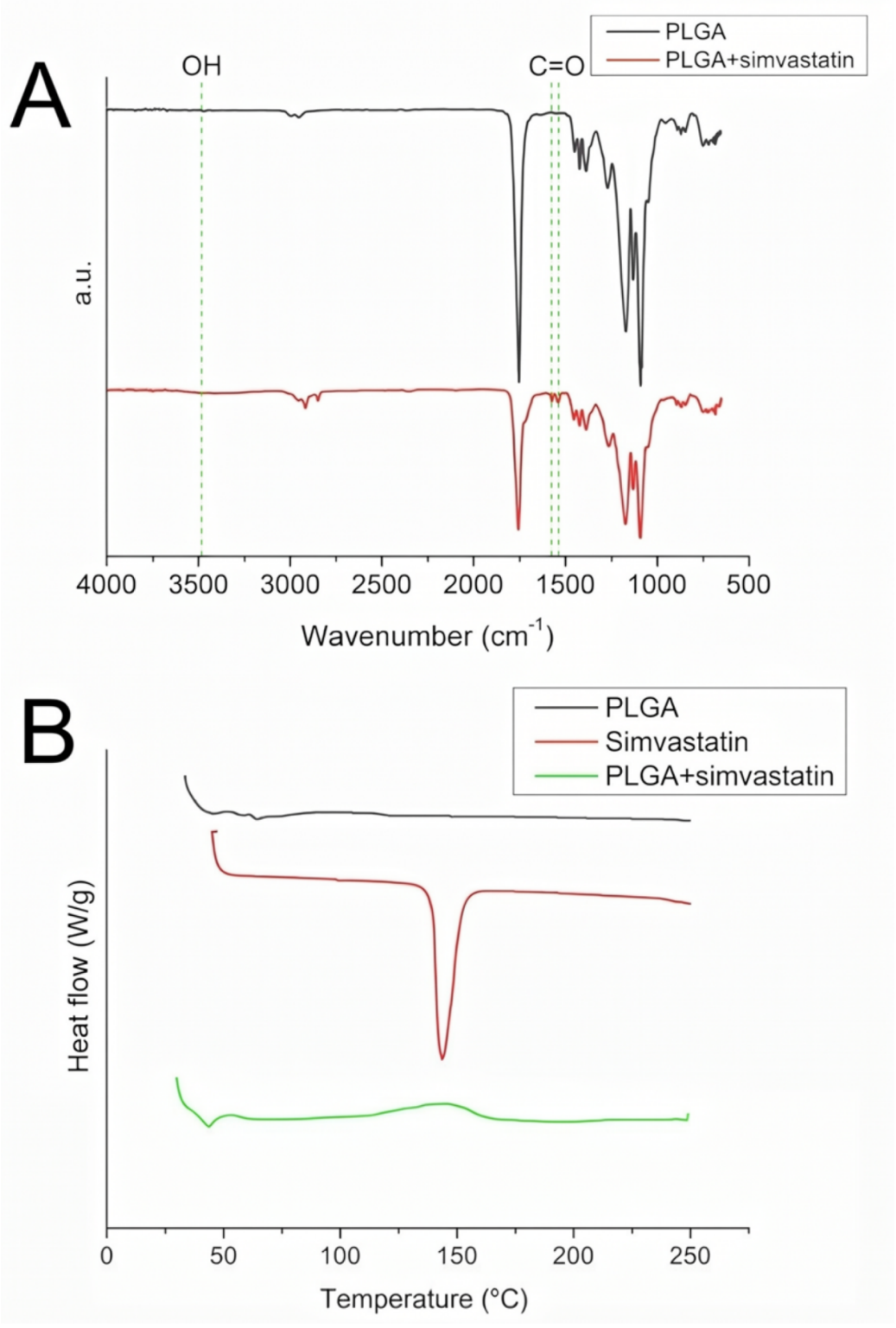


Figure 8. Fourier transform infrared (FTIR) spectra and thermal analysis of drug-loaded electrospun poly(lactic-co-glycolic acid) (PLGA) nanofibers. (A) FTIR spectra and (B) differential scanning calorimetry thermograms of pure PLGA, simvastatin, and simvastatin-loaded nanofibers.

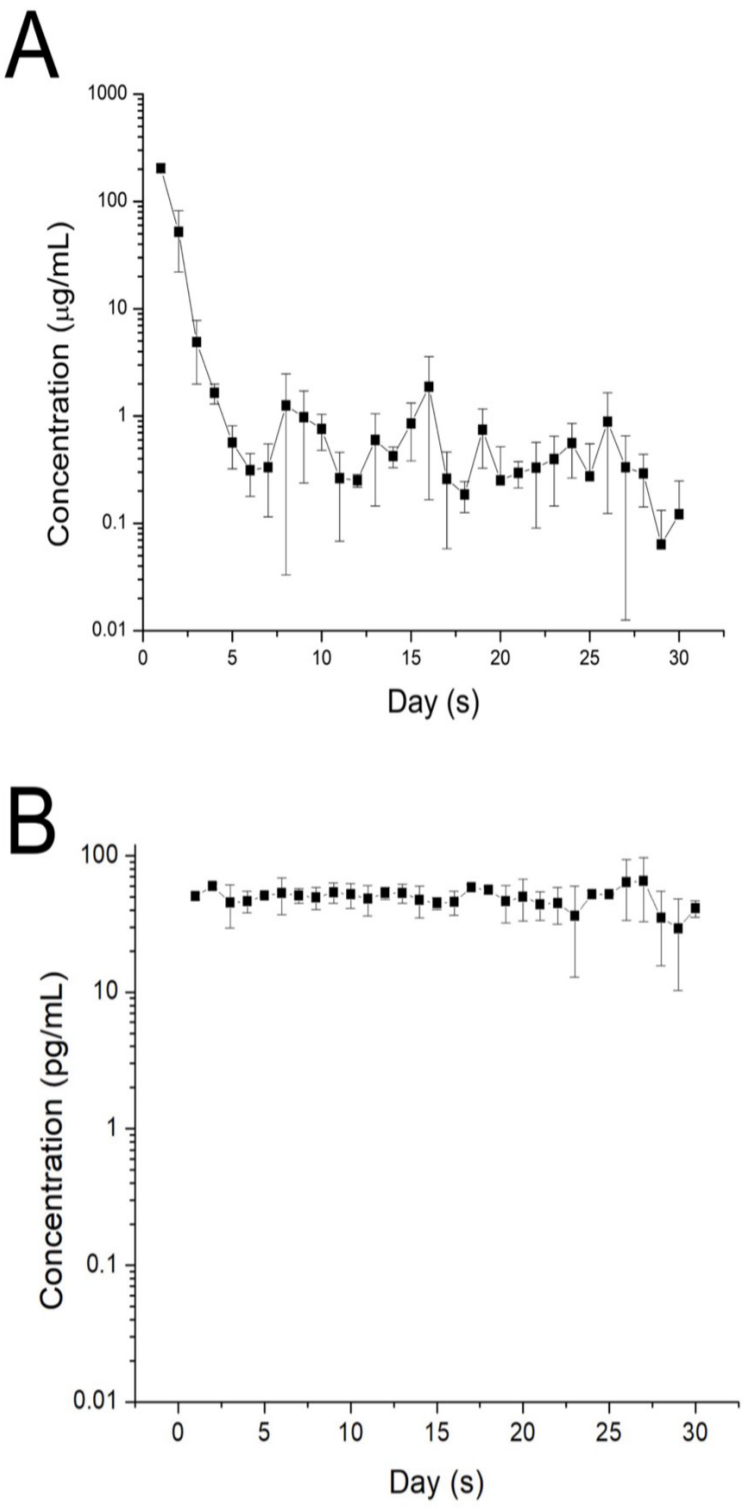


Figure 9. *In vitro* daily elution profiles of (A) simvastatin and (B) bone morphogenetic protein 2 from the nanofibers

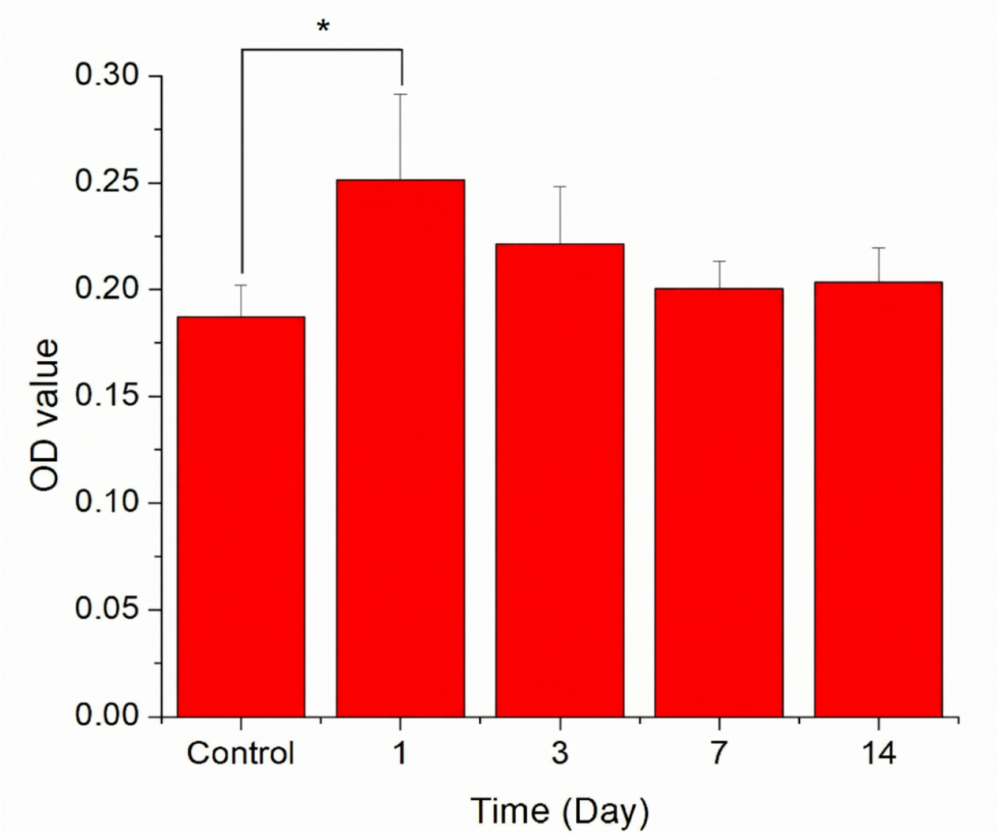


Figure 10. Cytotoxicity of drug-eluting nanofibers (*$p < 0.05$, relative to the control)
Abbreviation: OD: Optical density.

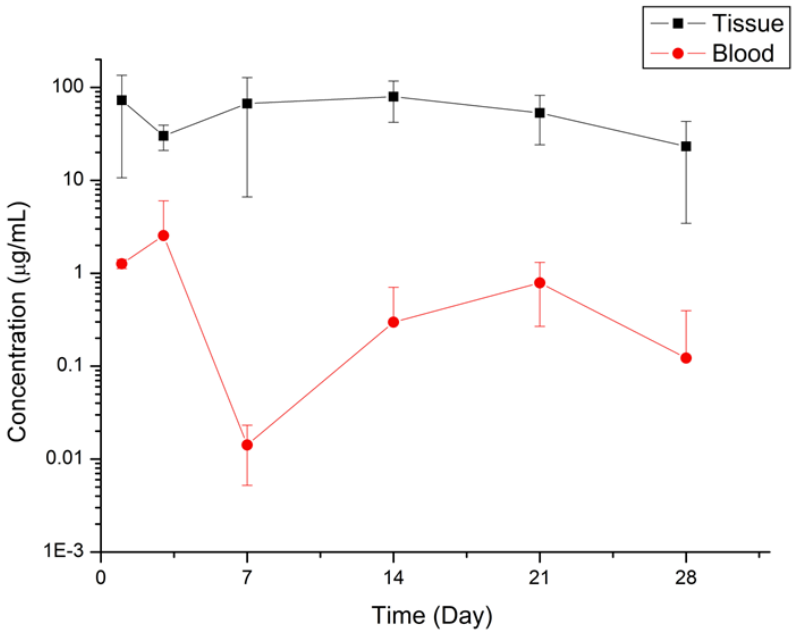


Figure 11. *In vivo* elution profile of simvastatin from drug-loaded pedicle screws

in blood flow. Additionally, the qualitative histological examination in Figure 12 revealed intact tissue structure with no obvious foreign-body inflammatory reaction or tissue necrosis across all time points.

4. Discussion

Pedicle screw loosening remains a significant challenge in bone fixation, particularly in spinal surgery, as it compromises implant stability and success. This study proposed biodegradable anchors to improve the pullout strength of pedicle screws in bone fixation using additive manufacturing and coaxial electrospinning techniques. The bioresorbable anchors degrade over time, allowing natural bone ingrowth to replace the membranes and thereby support long-term fixation. Additionally, when integrated with drug-eluting nanofibers, the anchors also enable the sustained release of pharmaceuticals and growth factors to promote bone healing.

Additive manufacturing (3D printing) enables the automated construction of customized, three-dimensional structures directly from computer-aided design models through layer-by-layer deposition.[18,19] In biomedical engineering, this approach allows precise control over implant geometry and porosity. Simultaneously, coaxial electrospinning offers a versatile platform for producing core–shell nanofibers by extruding two immiscible fluid streams through concentric nozzles under a high-voltage electric field.[20] A primary advantage of coaxial processing is its ability to shield labile protein therapeutics (e.g., BMP-2) within the protective core matrix while maintaining active drug molecules (e.g., simvastatin) in the outer sheath to tailor distinct, multi-stage release profiles.[21]

The experimental data in Figure 4A reveal that, in the cortical-bone analog, the bare screw showed the highest peak pullout force, followed closely by the nanofiber-wrapped screw. This was followed by the nylon anchor, while the additively manufactured PLA anchors showed substantially lower pullout forces. For cancellous bones (Figure 4B), the nanofibrous membrane again demonstrated the highest pullout strength, surpassing that of the bare screw. The nylon anchor showed pullout strengths comparable to the bare screws, whereas the PLA anchors once again exhibited substantially lower pullout strengths for the inserted pedicle screws.

The effectiveness of an anchor depends on its flexibility and extensibility. Electrospun nanofibers demonstrate exceptional flexibility and extensibility, allowing the nanofibrous membrane to fill microcavities between the bone and the inserted screws. This characteristic minimizes micro-movements at the bone–screw interface, particularly in cancellous bones with larger pores. Furthermore, the nylon anchor exhibits greater flexibility compared to the PLA anchors, enabling it to effectively redistribute excessive or uneven stress on the screw caused

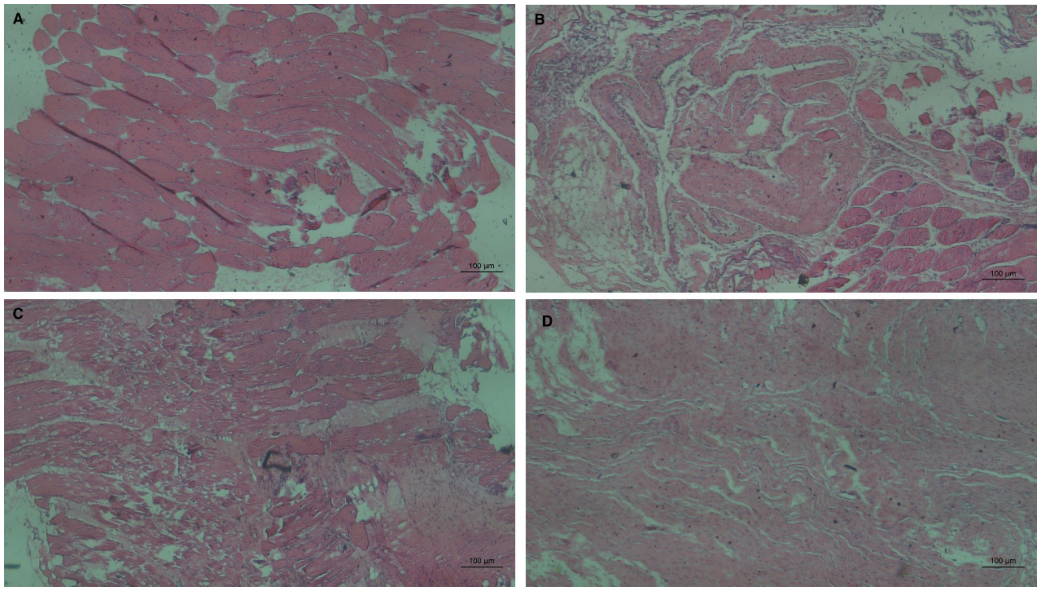


Figure 12. Histological evaluation of localized tissue compatibility around implanted pedicle screws over time. Representative histological images at (A) 1 day, (B) 7 days, (C) 14 days, and (D) 28 days post-implantation, demonstrating favorable local tissue response with intact cellular integrity and absence of localized tissue necrosis or overt inflammatory reactions. Scale bar: 100 μm; magnification: 100×.

by load-bearing activities or misalignment. As a result, the nylon anchor provides a higher pullout strength than the PLA anchors for the screw. By contrast, the PLA anchors exhibit high stiffness and may fracture during the screw-tightening process during insertion (Figure 2C). This prevents them from reducing excessive or uneven stress on the screw and does not contribute to increased pullout strength. To address the high stiffness and susceptibility to brittle fracture observed in PLA anchors, alternative biodegradable polymers such as PCL or PCL/PLA blends offer significant advantages. Mechanically, PCL exhibits a much lower glass transition temperature (Tg ≈ −60 °C) compared to PLA (Tg ≈ 60 °C), providing superior ductility and high elongation-at-break, which enables the anchor to deform plastically and absorb hoop stresses during screw tightening without structural splitting. Regarding degradation kinetics, PCL undergoes significantly slower hydrolytic degradation (2–3 years) than PLA (1–2 years) due to its higher hydrophobicity and semicrystalline structure. This prolonged degradation profile can maintain mechanical integrity over an extended period to support progressive bone ingrowth.

It should be emphasized that the synthetic bone block models (rigid polyurethane foam) were utilized specifically to provide a standardized, highly reproducible testing platform to evaluate the immediate, time-zero mechanical fixation performance of the screw–anchor systems while eliminating specimen-to-specimen variability inherent to biological cadaveric bone. We fully recognize that synthetic blocks cannot replicate the heterogeneous microarchitecture, variable bone mineral density, or dynamic biological remodeling and osseointegration processes of osteoporotic bone. Consequently, the superior pullout strength observed in the screw/nanofiber group (Figure 4B) reflects the immediate physical micro-filling and interlocking effect of the resilient nanofibrous membrane within interfacial micro-voids, rather than drug-induced biological bone regeneration.

Using therapeutic agents to prevent screw loosening is crucial for enhancing the longevity and success of orthopedic implants, particularly in lower-quality bones, such as osteoporotic bone. Simvastatin, a widely used statin for lowering cholesterol, has been shown to stimulate osteoblast differentiation and enhance bone formation by upregulating the expression of BMP-2. When used in conjunction with exogenously applied BMP-2, a potent osteoinductive protein that promotes the recruitment and differentiation of progenitor cells into osteoblasts, the synergy between these agents amplifies bone regeneration. This combination not only accelerates new bone formation but also improves the quality and density of the regenerated tissue, offering promising applications in treating bone defects, fractures, and conditions like osteoporosis. The dual action of simvastatin's systemic effects and BMP-2's localized osteoinduction creates a robust framework for advanced bone healing strategies. The experimental data in Figure 9 demonstrate that the integrated nanofiber anchor/screw system provides sustained *in vitro* release of simvastatin and BMP-2 for over 30 days. In addition, it eluted high levels of simvastatin for four weeks *in vivo* (Figure 11), with no detectable cytotoxicity. This offers advantages in terms of improved screw pullout strength as well as sustained release for bone healing.

Surface wettability strongly governs initial biological responses upon implantation, directly affecting protein adsorption and subsequent cell attachment.[22] Hydrophilic biomaterial surfaces enhance cell adhesion and spreading, establishing a favorable microenvironment for osteoblast proliferation and tissue integration.[23] Pure PLGA electrospun meshes exhibited hydrophobic behavior (water contact angle ~136.4°). However, the incorporation of simvastatin decreased the water contact angle from 136.4° to 100.6°, indicating reduced surface hydrophobicity, thereby facilitating fluid uptake and cellular interactions at the implant interface.

The *in vitro* elution kinetics of simvastatin from the electrospun nanofibers exhibited a biphasic profile, characterized by an initial burst release (~1,000 μg/mL on day 1) followed by a sustained low-level maintenance release (1–10 μg/mL) for over 30 days.[24] During coaxial electrospinning, while most simvastatin was embedded within the sheath PLGA matrix, a fraction of the drug likely resided near the fiber surface, contributing to the initial surge. Following this rapid surface diffusion, drug release was governed by combined matrix degradation and diffusion mechanisms, resulting in a steady, low-concentration elution profile.[24] In contrast, BMP-2 was encapsulated within the inner core, where the protective PLGA sheath enabled a highly stable release (~50–80 pg/mL) without significant burst fluctuations throughout the 30-day evaluation period.[25]

Clinically, an initial burst effect presents both therapeutic advantages and potential safety concerns. On one hand, a rapid early influx of simvastatin can suppress acute post-implantation inflammatory cascades and immediately upregulate local endogenous BMP-2 expression, effectively initiating osteogenic signaling during early bone remodeling. On the other hand, excessively high local drug concentrations carry cytotoxic risks. Notably, our *in vitro* MTT cell viability assay (Figure 10) and 4-week *in vivo* histological evaluations (Figure 12) confirmed intact cell viability and an absence of tissue necrosis, indicating

that the initial burst remained within a bio-tolerable range. Furthermore, *in vivo* pharmacokinetics (Figure 11) demonstrated that systemic blood concentrations remained minimal (<2.5 μg/mL), verifying that drug exposure was safely confined to the localized surgical site.

To better match the long-term biological timeline of bone healing, future material optimization strategies could focus on tailoring the release kinetics. This can be achieved by increasing the molecular weight of PLGA, utilizing higher lactide-to-glycolide ratios, incorporating hydrophobic PCL into the sheath layer, or adding a secondary drug-free barrier coating via electrospinning to suppress early surface diffusion and provide a more uniform, extended elution profile.

Although the nanofiber-wrapped screws and resorbable anchor designs demonstrated promising effectiveness, this study has several limitations. First, the relatively small number of animals may limit the generalizability of the findings. Second, healthy rabbit femur models and synthetic bone blocks were employed in this study, which may not fully reflect the clinical conditions associated with compromised bone quality. As a proof-of-concept investigation, the current work focused primarily on establishing the immediate mechanical feasibility and localized pharmacokinetic profiles of the hybrid system. However, synthetic blocks and normal bone conditions cannot capture the compromised bone quality or impaired healing capacity seen in clinical osteoporosis. Future studies utilizing an ovariectomized osteoporotic animal model combined with long-term micro-CT and histomorphometric evaluations are required to validate whether this drug-eluting system can enhance bone–implant integration and long-term stability under pathological conditions. Finally, future studies should explore other biodegradable polymers, such as PCL, PCL/PLA blends, and more flexible polymer systems, as potential materials for biodegradable anchors to further improve the pullout strength of pedicle screws.

5. Conclusion

We developed various biodegradable nanofibrous anchors loaded with simvastatin and BMP-2 to enhance the pullout strength of pedicle screws from artificial bones. Experimental results indicate that electrospun drug-eluting nanofibers, when wrapped around pedicle screws, improve their pullout strength. Moreover, the nanofiber/screw system ensures sustained simvastatin release for over 30 days *in vitro* and 4 weeks *in vivo*. Histological analysis further confirmed the biocompatibility of the resorbable nanofibers. These findings suggest that electrospun drug-eluting nanofibrous membranes can enhance immediate screw fixation and serve as an effective platform for prolonged drug delivery. Further quantitative histomorphometric evaluations and studies in pathological animal models are warranted prior to clinical translation.

Acknowledgments

None.

Funding

This work was supported in part by the National Science and Technology Council, Taiwan (Contract No. 111-2221-E-182-004-MY3) and the Chang Gung Memorial Hospital (Contract Nos. CMRPD2M0131 and CMRPD2M0012).

Conflict of interest

The authors declare they have no competing interests.

Author contributions

Conceptualization: Po-Ju Lai, Shih-Jung Liu
Formal analysis: Po-Ju Lai, Chien-Yun Yang, I-Lan Fan, Ching-Lung Tai
Methodology: Po-Ju Lai, Chih-Yang Lai, Ching-Lung Tai, Shih-Jung Liu
Investigation: Po-Ju Lai, Chih-Yang Lai, Chien-Yun Yang, I-Lan Fan
Writing–original draft: Po-Ju Lai
Writing–review & editing: Shih-Jung Liu, Ching-Lung Tai

Ethics approval and consent to participate

All animal-related experimental protocols were reviewed and approved by the Institutional Animal Care and Use Committee (IACUC) of Chang Gung University (Approval No.: CGU113-030). The study was conducted in strict accordance with the approved guidelines for the care and use of laboratory animals.

Consent for publication

Not applicable

Availability of data

The data that support the findings of this study are available from the corresponding author upon reasonable request.

References

1. Yuan L, Zhang X, Zeng Y, Chen Z, Li W. Incidence, risk, and outcome of pedicle screw loosening in degenerative lumbar scoliosis patients undergoing long-segment fusion. *Global Spine J*. 2023;13(4):1064-1071.

doi: 10.1177/21925682211017477

2. Wu Q, Huang J, Cao Y. Risk factors for pedicle screw loosening: a comprehensive review. *J Orthop Surg Res*. 2025;20(1):914.

doi: 10.1186/s13018-025-06349-z

3. Şahin ÖF, Uzlu O, Açıkgöz Hİ, *et al.* Pedicle screw loosening after lumbar spinal stenosis surgery and an analytical review of recurrent loosening: based on revision surgery experience. *Med Sci Monit*. 2026;32:e951549.

doi: 10.12659/MSM.951549

4. Huang YC, Liu PC, Lin HH, *et al.* Risk prediction model of pedicle screw loosening within 2 years after decompression and instrumented fusion surgery for degenerative lumbar disease. *Spine J*. 2025;25(7):1474-1482.

doi: 10.1016/j.spinee.2025.01.033

5. Yuan H, Liu Y, Dai C, *et al.* Predictive factors of distal pedicle screw loosening followed posterior corrective surgery for degenerative lumbar scoliosis. *BMC Musculoskelet Disord*. 2025;26(1):283.

doi: 10.1186/s12891-025-08519-w

6. Hsieh MK, Li YD, Li YC, Liu MY, Tsai TT, Lai PL, Tai CL. Improved fixation stability for repairing pedicle screw loosening using a modified cement filling technique in porcine vertebrae. *Sci Rep*. 2022;12(1):2739.

doi: 10.1038/s41598-022-06724-4

7. Peng J, Guo H, Zhan C, *et al.* Comparison of pedicle screw fixation with or without cement augmentation for treating single-segment isthmic spondylolisthesis in the osteoporotic spine. *Sci Rep*. 2023;13(1):827.

doi: 10.1038/s41598-023-27539-x

8. Wu X, Shi J, Cheng Y, *et al.* Pedicle screw loosening: the value of radiological imagings and the identification of risk factors assessed by extraction torque during screw removal surgery. *J Orthop Surg Res*. 2019;14(1):6.

doi: 10.1186/s13018-018-1046-0

9. McKoy BE, An YH. An expandable anchor for fixation in osteoporotic bone. *J Orthop Res*. 2001;19(4):545-547.

doi: 10.1016/S0736-0266(00)00052-8

10. Massaad E, Rolle M, Hadzipasic H, Kiapour A, Shankar GM, Shin JH. Safety and efficacy of cement augmentation with fenestrated pedicle screws for tumor-related spinal instability. *Neurosurg Focus*. 2021;50(5):E12.

doi: 10.3171/2021.2.FOCUS201121

11. Barnett E, Fletcher J, Gill HS, Pegg EC, Loukaides EG. Auxetic fixation devices can achieve superior pullout performances compared to standard fixation concepts. *Smart Mater Struct*. 2024;33(6):065010.

doi: 10.1088/1361-665X/ad442d

12. Lin CK, Jaw FS, Young TH. A novel UHMWPE anchor for improving the pullout resistance of pedicle screws. *Front Bioeng Biotechnol*. 2026;14:1741050.

doi: 10.3389/fbioe.2026.1741050

13. Chen Z. Non-concrete breakout failure modes of concrete mechanical anchors in tension-a literature review. *Constr Build Mater.* 2023;366:1301222.

doi: 10.1016/j.conbuildmat.2022.130222

14. Lee CH, Hsieh MJ, Roth J, *et al.* Hybrid core-shell nanofibrous scaffolds/stents delivery angiotensin II receptor blocker to treat diabetic artery disease. *ACS Appl Polym Mater*. 2022;4(6):4199-4207.

doi: 10.1021/acsapm.2c00186

15. Novakova L, Satinsky D, Solich P. HPLC methods for the determination of simvastatin and atorvastatin. *Trends Analyt Chem*. 2008;27(4):352-367.

doi: 10.1016/j.trac.2008.01.013

16. Hakiem AFA, Mohamed NA, Ali HRH. FTIR spectroscopic study of two isostructural statins: Simvastatin and Lovastatin as authentic and in pharmaceuticals. *Spectrochim Acta A Mol Biomol Spectrosc*. 2021;261:120045.

doi: 10.1016/j.saa.2021.120045

17. Karolewicz B, Gajda M, Owczarek A, Pluta J, Górniak A. Physicochemical and dissolution studies of simvastatin solid dispersions with Pluronic F127. *Pharmazie*. 2014;69(8):589-594.

doi: 10.1691/ph.2014.3217

18. Kanishka K, Acherjee B. Revolutionizing manufacturing: a comprehensive overview of additive manufacturing processes, materials, developments, and challenges. *J Manuf Process*. 2023;107:574-619.

doi: 10.1016/j.jmapro.2023.10.024

19. Ngo TD, Kashani A, Imbalzano G, Nguyen KT, Hui D. Additive manufacturing (3D printing): a review of materials, methods, applications and challenges. *Compos B Eng*. 2018;143:172-196.

doi: 10.1016/j.compositesb.2018.02.012

20. Bazilevsky AV, Yarin AL, Megaridis CM. Co-electrospinning of core-shell fibers using a single-nozzle technique. *Langmuir*. 2007;23(5):2311-2314.

doi: 10.1021/la063194q

21. Khan J, Khan A, Khan MQ, Khan H. Applications of co-axial electrospinning in the biomedical field. *Next Mater*. 2024;3:100138.

doi: 10.1016/j.nxmate.2024.100138

22. Ehtesabi H, Massah F. Improvement of hydrophilicity and cell attachment of polycaprolactone scaffolds using green synthesized carbon dots. *Mater Today Sustain*. 2021;13:100075.

doi: 10.1016/j.mtsust.2021.100075

23. Zhou J, Akrami N, Wang H, *et al.* Enhanced healing of critical-sized bone defects using degradable scaffolds with tailored composition through immunomodulation and angiogenesis. *Bioact Mater*. 2025;44:371-388.

    doi: 10.1016/j.bioactmat.2024.10.018

24. Ali SA, Doherty PJ, Williams DF. Mechanisms of polymer degradation in implantable devices. 2. Poly(DL-lactic acid). *J Biomed Mater Res*. 1993;27(11):1409-1418.

    doi: 10.1002/jbm.820271108

25. Kamaly N, Yameen B, Wu J, Farokhzad OC. Degradable controlled-release polymers and polymeric nanoparticles: mechanisms of controlling drug release. *Chem Rev*. 2016;116(4):2602-2663.

    doi: 10.1021/acs.chemrev.5b00346